Combined deletion of Vhl, Trp53 and Kif3a causes cystic and neoplastic renal lesions

Guinot, Anna ; Lehmann, Holger ; Wild, Peter J ; Frew, Ian J

Abstract: The von Hippel-Lindau (VHL) tumour suppressor gene is biallelically inactivated in the majority of cases of clear cell renal cell carcinoma (ccRCC), however Vhl knockout mouse models do not recapitulate human ccRCC, implying that additional mutations are required for tumour formation. Mutational inactivation of VHL sensitises renal epithelial cells to lose the primary cilium in response to other mutations or extracellular stimuli. Cilia loss is believed to represent a second hit in VHL mutant cells that causes the development of cystic lesions that in some cases can progress to ccRCC. Supporting this idea, genetic ablation of the primary cilium by deletion of the kinesin family member 3A (Kif3a) gene cooperates with loss of Vhl to accelerate cyst formation in mouse kidneys. Additionally, aged Vhl/Trp53 double mutant mice develop renal cysts and tumours at a relatively low incidence, suggesting that there is a genetic cooperation between VHL and TP53 mutation in the development of ccRCC. Here we generated renal epithelium-specific Kif3a/Trp53 and Vhl/Kif3a/Trp53 mutant mice to investigate whether primary cilium deletion would accelerate the development of cystic precursor lesions or cause their progression to ccRCC. Longitudinal microcomputed tomography imaging and histopathological analyses revealed an increased rate of cyst formation, increased proportion of cysts with proliferating cells, higher frequency of atypical cysts as well as the development of neoplasms in Vhl/Kif3a/Trp53 mutant kidneys compared to Kif3a/Trp53 or Vhl/Kif3a mutant kidneys. These findings demonstrate that primary cilium loss in addition to Vhl and Trp53 losses promotes the transition towards malignancy and provide further evidence that the primary cilium functions as a tumour suppressor organelle in the kidney.

DOI: https://doi.org/10.1002/path.4736

Combined deletion of *Vhl*, *Trp53* and *Kif3a* causes cystic and neoplastic renal lesions

Anna Guinot[1], Holger Lehmann[1], Peter J. Wild[2] and Ian J. Frew[1,3*]

[1] Institute of Physiology, University of Zurich, Zurich, Switzerland

[2] Institute of Surgical Pathology, University Hospital Zurich, Zurich, Switzerland

[3] Zurich Center for Integrative Human Physiology, University of Zurich, Zurich, Switzerland

**** Correspondence to*** *Ian Frew, Institute of Physiology, University of Zurich, Winterthurerstrasse 190, CH-8057 Zurich, Switzerland. e-mail: ian.frew@access.uzh.ch*

Conflict of interest: The authors declare that there are no conflicts of interest related to this manuscript.

This article has been accepted for publication and undergone full peer review but has not been through the copyediting, typesetting, pagination and proofreading process, which may lead to differences between this version and the Version of Record. Please cite this article as doi: 10.1002/path.4736

Abstract

The von Hippel-Lindau (VHL) tumour suppressor gene is biallelically inactivated in the majority of cases of clear cell renal cell carcinoma (ccRCC), however *Vhl* knockout mouse models do not recapitulate human ccRCC, implying that additional mutations are required for tumour formation. Mutational inactivation of *VHL* sensitises renal epithelial cells to lose the primary cilium in response to other mutations or extracellular stimuli. Cilia loss is believed to represent a second hit in *VHL* mutant cells that causes the development of cystic lesions that in some cases can progress to ccRCC. Supporting this idea, genetic ablation of the primary cilium by deletion of the kinesin family member 3A (*Kif3a*) gene cooperates with loss of *Vhl* to accelerate cyst formation in mouse kidneys. Additionally, aged *Vhl/Trp53* double mutant mice develop renal cysts and tumours at a relatively low incidence, suggesting that there is a genetic cooperation between *VHL* and *TP53* mutation in the development of ccRCC. Here we generated renal epithelium-specific *Kif3a/Trp53* and *Vhl/Kif3a/Trp53* mutant mice to investigate whether primary cilium deletion would accelerate the development of cystic precursor lesions or cause their progression to ccRCC. Longitudinal microcomputed tomography imaging and histopathological analyses revealed an increased rate of cyst formation, increased proportion of cysts with proliferating cells, higher frequency of atypical cysts as well as the development of neoplasms in *Vhl/Kif3a/Trp53* mutant kidneys compared to *Kif3a/Trp53* or *Vhl/Kif3a* mutant kidneys. These findings demonstrate that primary cilium loss in addition to *Vhl* and *Trp53* losses promotes the transition towards malignancy and provide further evidence that the primary cilium functions as a tumour suppressor organelle in the kidney.

Key words

Clear cell renal cell carcinoma, von Hippel-Lindau, primary cilium, Trp53, mouse model

Introduction

Clear cell renal cell carcinoma (ccRCC) is the most common type of renal cancer, accounting for approximately 70% of all cases [1]. The von Hippel-Lindau (*VHL*) tumour suppressor gene is biallelically inactivated in over 90% of sporadic cases of ccRCC [2]. Inheritance of a mutant allele of the *VHL* gene results in the autosomal dominant VHL syndrome, which is characterised not only by the development of ccRCC but also by renal and pancreatic cysts as well as tumours in the central nervous system, retina, pancreas and ear [3-5]. Kidneys of patients with VHL disease exhibit a range of lesions that likely represent precursors of ccRCC [3], including simple cysts that are lined by a single layer of epithelial cells and atypical cysts that display multi-layered epithelial structures that resemble small foci of ccRCC growing in the wall of the cyst. It has been shown that the growth of these tumour cells in a subset of atypical cysts may fill the cystic lesion to generate a solid ccRCC or a solid ccRCC with a cystic component [6]. About 5% of all *VHL* mutant ccRCCs occurring sporadically lack a solid tumour component and are classified as multilocular multicystic renal cell carcinomas in which clear cell tumour cells grow within and between the walls of multiple cysts. The growth pattern of this neoplasm of low malignant potential is reminiscent of the appearance of atypical cysts in VHL patients, suggestive of a cystic origin of this tumour entity. However, while the transition from a cystic lesion to a solid ccRCC has been observed to occur at low frequency in longitudinal imaging studies of VHL patients, the majority of large cystic lesions do not develop into solid ccRCCs within a short timeframe [6] implying that not all cysts have the propensity to develop into ccRCCs. Additionally, small solid micro-ccRCC lesions can be observed in histological sections of VHL patient kidneys and longitudinal imaging studies of VHL patients demonstrate the growth of solid ccRCCs from small solid lesions [6]. Thus, the initiation of ccRCC can occur from a cystic precursor lesion or a solid precursor lesion [7, 8].

The loss of function of the pVHL protein alone is insufficient to induce ccRCC formation despite being necessary for the growth of established *VHL*-mutant ccRCC cell lines in mouse xenograft assays [9]. On one hand, ccRCC arises relatively infrequently in kidneys of patients with VHL disease considering the vast number of *VHL* null cells that these kidneys contain [10] and on the other hand, none of the many *Vhl* knockout mouse models that have been generated developed renal tumours [3]. These arguments support the hypothesis that additional genetic mutations act in cooperation with the loss of *VHL* in causing tumour formation.

One of pVHL's many biological functions is stabilisation of the microtubule core of the primary cilium, a microtubule-based organelle that acts as a sensor of chemical and mechanical signals [11]. Loss of functionality or structure of the primary cilium causes polycystic diseases in the kidney [12]. Cystic lesions in VHL patients exhibit a reduced frequency of ciliated epithelial cells [13] and cells of human ccRCCs have a very low frequency of primary cilia in comparison to normal renal epithelia and in comparison to other types of renal cell carcinoma [14]. However, *Vhl* knockout in renal epithelial cells is not sufficient to cause loss of the primary cilium *in vivo* [13]. Rather, loss of pVHL function sensitises cells to lose the primary cilium in response to cellular signals that lead to inactivation of GSK3β [13]. The *PTEN* tumour suppressor gene is genetically inactivated in approximately 5% of human ccRCCs [2, 15]. Constitutive activation of the PI3K signalling pathway via deletion of *Pten* leads to inactivation of GSK3β and when combined with deletion of *Vhl* causes a reduction in the frequency of ciliated epithelial cells and leads to cyst formation in mouse kidneys [16]. These findings argue that secondary genetic mutations or signalling alterations can cause *VHL* mutant cells to lose the primary cilium, initiating cystic lesions that can potentially lead to ccRCC [16].

This idea has recently been further supported by studies investigating genetic ablation of the primary cilium in the kidney. Kinesin family member 3A (*Kif3a*) is a component of the kinesin-II microtubule motor complex and its deletion prevents the formation of the primary cilium in cells and leads to cyst formation in mouse kidneys [17]. Co-deletion of *Vhl* and *Kif3a* accelerates cyst initiation and increases the total number of cysts per kidney as well as the frequency of atypical cysts [18]. However, because these atypical cysts did not form tumours it is likely that additional genetic alterations are required for progression to ccRCC.

Analyses of single biopsies of human ccRCC revealed that the *TP53* tumour suppressor gene is mutated in 2-8% of ccRCCs [2, 15, 19] and that genetic alterations in regulators of p53, including *MDM2*, *ATM*, *CHEK2* and *CDKN2A* occur mutually exclusively to *TP53* mutations, arguing that the p53 pathway is functionally altered in approximately 20-25% of ccRCCs [2]. Analyses of 10 ccRCCs by sequencing multiple biopsies from different regions of each tumour revealed that 40% of these tumours harboured *TP53* mutations in at least one tumour region, implying that the large scale tumour sequencing studies have likely underestimated the frequency of *TP53* mutations that can be present in spatially distinct sub-clonal populations within ccRCC tumours [20]. Supporting the functional relevance of p53 pathway alteration in ccRCC, co-deletion of *Vhl* with *Trp53* in the mouse renal epithelium not only led to the formation of simple and atypical cystic lesions but also to tumours that share several histological and molecular similarities with ccRCC [19]. Since *Vhl/Trp53* double mutant mice developed cysts and tumours with late onset and with relatively few lesions per kidney and since *Vhl/Kif3a* double mutant mice developed many cysts within a few months of gene deletion we generated a mouse model that combines the mutation of *Vhl*, *Trp53* and *Kif3a* to ask whether loss of these tumour suppressors together with ablation of the primary cilium might lead to the formation of ccRCC.

Materials and Methods

Animals

Mice expressing a tamoxifen-inducible kidney-specific Cre recombinase under the Ksp1.3 promoter [21] were crossed with *Kif3a*$^{fl/fl}$, *Vhl*$^{fl/fl}$ and/or *Trp53*$^{fl/fl}$ animals [18,19]. To achieve gene deletion 6-week old mice were fed with tamoxifen-containing food (Harlan Laboratories) for 2 weeks. Non-Cre transgenic littermates were used as controls. Mouse experiments were conducted under experimental license 131/2012 from the Veterinary Office of the Canton of Zurich.

Genomic DNA isolation and sequencing

Formalin-fixed, paraffin embedded kidney sections were dipped in Xylol for 5 minutes and then air-dried. Tissue was scratched off the slides and genomic DNA was isolated with the Arcturus PicoPure DNA Extraction Kit (Life Technologies). Sequences of the primers used for detecting the recombined alleles and the S6 internal control are given in the Supplementary Information.

Microcomputed tomography (µCT) imaging

Intravenous injections of Visipaque 270 (GE Healthcare) were performed at 8µl/g of body weight [22]. Images were obtained with a Quantum FX microCT (Perkin Elmer) with the following settings: 100 µA, 90 kV, respiratory gating and fine scanning.

Immunohistochemistry and immunofluorescence

Immunohistochemistry and immunofluorescence were conducted using previously described methods [18] with the following antibodies to: acetylated tubulin (T6793; Sigma-Aldrich), cleaved Caspase 3 (9661; Cell Signaling), HIF-1α (NB100-105; Novus Biologicals), Ki67 (M7248; Dako), P-4E-BP1 (Thr37/46) (2855; Cell Signaling), P-ERK1/2 (Thr202/Tyr204)

(9101; Cell Signaling), Pbrm1 (A-301-591A; Bethyl Laboratories) and Tri-Methyl-Histone H3 (Lys36) (4909; Cell Signaling). The secondary antibodies used were: goat anti-mouse Alexa 488 (A-11001; Life Technologies and horseradish peroxidase-coupled anti-mouse (31430; ThermoFisher Scientific).

Results

To investigate the consequences of combined *Vhl*, *Trp53* and *Kif3a* deletion in the mouse renal epithelium we generated Ksp1.3-Cre$^{ERT2\ Tg/+}$; Kif3a$^{fl/fl}$; Vhl$^{fl/fl}$; Trp53$^{fl/fl}$ and Ksp1.3-Cre$^{ERT2\ Tg/+}$; Kif3a$^{fl/fl}$; Trp53$^{fl/fl}$ mice. Non-transgenic (Ksp1.3-Cre$^{ERT2\ +/+}$) littermates were used as controls. All mice were fed tamoxifen-containing food at 6 weeks of age for 2 weeks to induce Cre activation. We chose this protocol as we have previously empirically determined that it allows a moderate level of gene deletion that leads to a moderate number of lesions, allowing the mice to be aged for as long as possible before the presence of many and large cysts might impair renal function. Hereafter control mice are referred to as Kif3a$^{fl/fl}$;Vhl$^{fl/fl}$;Trp53$^{fl/fl}$ or Kif3a$^{fl/fl}$;Trp53$^{fl/fl}$ and transgenic mice as Kif3a$^{\Delta/\Delta}$;Vhl$^{\Delta/\Delta}$;Trp53$^{\Delta/\Delta}$ or Kif3a$^{\Delta/\Delta}$;Trp53$^{\Delta/\Delta}$. Deletion of both or all three genes in the respective kidneys was confirmed by recombination-specific PCR of genomic DNA (Figure 1A). *Vhl* null cells are commonly identified by nuclear accumulation of hypoxia-inducible factor 1-α (HIF-1α) [16] whilst functional *Kif3a* deletion can be determined by the absence of primary cilia detected by loss of staining for acetylated tubulin, which normally stains primary cilia very strongly [17]. p53 is not detectable in normal renal cells and its loss can therefore not be assessed by immunohistochemistry [19]. All cystic epithelial cells lacked primary cilia in both genotypes (Figure 1B) whilst HIF-1α nuclear staining was present solely in Kif3a$^{\Delta/\Delta}$;Vhl$^{\Delta/\Delta}$;Trp53$^{\Delta/\Delta}$ and not in Kif3a$^{\Delta/\Delta}$;Trp53$^{\Delta/\Delta}$ epithelial cells of cysts (Figure 1B), functionally confirming the deletions of *Kif3a* and *Vhl*. Additionally, in Kif3a$^{\Delta/\Delta}$;Vhl$^{\Delta/\Delta}$;Trp53$^{\Delta/\Delta}$ kidneys we frequently observed histologically normal renal tubules that contained single or multiple cells that displayed strong nuclear accumulation of HIF-1α (data not shown) indicative of Cre activation during the period of tamoxifen feeding.

This observation argues that not all mutant cells form lesions and that the frequency of gene deletion is not a limitation to the formation of lesions.

We monitored renal cyst development in each animal over time via microcomputed tomography (μCT). Animals under anaesthesia received an intravenous injection of a contrast agent that permits visualisation of the kidneys in μCT imaging due to the concentration of the contrast agent in the renal tubular fluid [18, 22]. Cysts or other lesions fail to concentrate the contrast agent and are displayed as dark areas in the images [18, 23]. Mice were imaged every 4 weeks post-tamoxifen treatment for 40 weeks and kidneys were isolated after the last imaging (Figure 2). In a few cases in which the cystic burden was very high the mice were sacrificed at earlier timepoints. Cysts were observed in all transgenic animals (Figures 2B and 2C) whilst control animals did not develop any cysts (Figure 2A). The cystic burden observed in histological sections of whole kidneys correlated with the μCT imaging (Figures 2A, 2B and 2C). Both genotypes exhibited mainly a moderate cystic phenotype but some mice developed a severe cystic phenotype. This inter-animal variation is most likely due to variations in the efficiency of tamoxifen-induced Cre activation. Compared to $Kif3a^{\Delta/\Delta};Trp53^{\Delta/\Delta}$ mice the $Kif3a^{\Delta/\Delta};Vhl^{\Delta/\Delta};Trp53^{\Delta/\Delta}$ mice developed cysts at an earlier age (Figure 2D). The onset of cyst formation in $Kif3a^{\Delta/\Delta};Vhl^{\Delta/\Delta};Trp53^{\Delta/\Delta}$ mice was almost identical to the onset seen in our previous studies with $Kif3a^{\Delta/\Delta};Vhl^{\Delta/\Delta}$ mice while the onset in $Kif3a^{\Delta/\Delta};Trp53^{\Delta/\Delta}$ mice was faster and more penetrant than seen previously in $Kif3a^{\Delta/\Delta}$ mice [18]. However, analysis of histological sections showed that both genotypes harboured equivalent numbers of cysts per kidney section at the end time point (Figure 2E).

Histological analyses revealed that both genotypes predominantly developed simple cysts (Figures 3A and 3E), which are lined by a single layer of epithelial cells. Some cystic lesions in kidneys of VHL patients display an atypical morphology characterised by a multi-layered epithelium or epithelial projections into the cystic lumen. These atypical cysts are considered to be pre-malignant lesions. Similar lesions were observed in $Kif3a^{\Delta/\Delta};Vhl^{\Delta/\Delta};Trp53^{\Delta/\Delta}$ mice (Figures 3F) and more rarely in $Kif3a^{\Delta/\Delta};Trp53^{\Delta/\Delta}$ mice (Figures 3B and 3C). Moreover, in comparison to $Kif3a^{\Delta/\Delta};Trp53^{\Delta/\Delta}$ mice and the previously published $Kif3a^{\Delta/\Delta};Vhl^{\Delta/\Delta}$ mice [18], $Kif3a^{\Delta/\Delta};Vhl^{\Delta/\Delta};Trp53^{\Delta/\Delta}$ animals developed lesions that appeared to represent a further step in the process of malignant progression including cysts with larger neoplastic projections (Figures 3G and 3H) and occasional small solid neoplasms (Figures 3I and 3J). These neoplastic lesions were between 50 and 250 μm in diameter. In comparison to normal renal epithelial cells (Figure 3K) the cells in atypical cysts and neoplasms displayed weak cytoplasmic eosin staining and a clear cell appearance that is similar to the appearance of clear cell tumour cells in ccRCC (Figure 3L-N). While it appears likely that simple cysts, atypical cysts and neoplasms represent a continuous spectrum of lesions, for the purposes of quantification we defined atypical cysts to be cysts in which the maximum thickness of multi-layered cellular growth was three cells deep and collectively termed lesions in which cellular growths contained four or more cell layers (either cystic lesions or solid lesions) as neoplasms. These analyses demonstrated an increased proportion of both atypical cysts and of neoplasms in $Kif3a^{\Delta/\Delta};Vhl^{\Delta/\Delta};Trp53^{\Delta/\Delta}$ animals (approximately 15% combined) compared to $Kif3a^{\Delta/\Delta};Trp53^{\Delta/\Delta}$ animals (approximately 5% combined) (Figure 3O). In comparison, the percentage of atypical cysts seen in our previous studies of $Kif3a^{\Delta/\Delta}$ and $Kif3a^{\Delta/\Delta};Vhl^{\Delta/\Delta}$ mice were 2% and 8% respectively [18]. Thus, the triple mutant combination

greatly increases the number of cysts that display atypical and neoplastic epithelial linings. We conclude that triple deletion of *Kif3a*, *Vhl* and *Trp53* in kidney epithelial cells *in vivo* reproduces the proposed model of cystic ccRCC progression where simple cysts evolve to atypical cysts and then on to neoplasms.

Cysts in VHL patient kidneys and human ccRCC frequently display activation of mTORC1 signalling [2, 15, 16]. Primary cilia have also been implicated in the regulation of PI3K-mTORC1 signalling [24, 25]. Immunohistochemical staining using an antibody against phosphorylated Thr37/Thr46-4E-BP1, a readout of mTORC1 activation, revealed that cysts in $Kif3a^{\Delta/\Delta};Vhl^{\Delta/\Delta};Trp53^{\Delta/\Delta}$ kidneys displayed more frequent phosphorylation of 4E-BP1 than cysts in $Kif3a^{\Delta/\Delta};Trp53^{\Delta/\Delta}$ kidneys (Figures 4A and 4C). A similar result was obtained with analysis of phosphorylated Thr202/Tyr204-ERK1/2, which is activated downstream of numerous growth factor signalling pathways (Figures 4B and 4D). We next asked whether the increased activation of these pro-proliferative signalling pathways was associated with increased proliferation of cystic cells by staining histological sections of mice with comparable moderate phenotypes with an antibody against Ki67, a marker of proliferative cells. This staining revealed a mixture of cysts with and without proliferating cells (Figure 4G). Quantification of Ki67 positive (Ki67+) cysts revealed twice as many proliferating cysts in $Kif3a^{\Delta/\Delta};Vhl^{\Delta/\Delta};Trp53^{\Delta/\Delta}$ kidneys as in $Kif3a^{\Delta/\Delta};Trp53^{\Delta/\Delta}$ kidneys (Figure 4E). However, no differences were observed between the two genotypes in relation to the frequency of Ki67+ cells within proliferating cysts (Figure 4F). There were no differences between genotypes in the extent of apoptosis as measured by nuclear immunoreactivity using an antibody against cleaved (activated) caspase 3 (Figures 4H and 4I). These data show that triple mutant cysts are more likely to be proliferating and growing than the double mutant cysts and this may contribute to the enhanced transition to a more malignant phenotype.

Since atypical cysts and neoplasms arise less frequently than simple cysts it is possible that additional genetic alterations may have occurred in these cells to cause this transition to a more neoplastic phenotype. Inactivating mutations in *PBRM1*, *BAP1* and *SETD2* arise frequently in human ccRCC [2, 15]. While the microscopic nature of the neoplastic lesions in $Kif3a^{\Delta/\Delta};Vhl^{\Delta/\Delta};Trp53^{\Delta/\Delta}$ kidneys prevented genetic analyses, we utilised immunohistochemistry to assess potential genetic deletion or truncation of *Pbrm1* using an antibody against PBRM1. We assessed potential inactivating mutations of *Setd2* using an antibody against histone H3 trimethylated lysine 36 (H3K36me3), a protein modification that is entirely dependent on SETD2 function. A functioning antibody against mouse BAP1 is not commercially available. These studies revealed PBRM1 and H3K36me3 immunoreactivity in all simple cysts, atypical cysts and neoplasms (Supplementary Figures 1A and 1B) arguing against the deletion or mutation of these genes as being a contributing factor in the evolution of these lesions.

Discussion

We recently showed that combined deletion of *Vhl* and *Kif3a* accelerates renal cyst formation and increases the total number of cysts and the proportion of atypical cysts when compared with *Kif3a* deletion alone [18]. We argued that loss of the primary cilium cooperates with loss of pVHL function to promote cyst formation and that additional mutations are likely to be required to progress toward ccRCC via a cyst-dependent pathway. Previously we also showed that combined deletion of *Vhl* and *Trp53* in mice leads to the formation of simple and atypical cysts as well as tumours in the kidneys [19]. However, limitations of the *Vhl/Trp53* model were the low incidence and long latency of tumour formation (1 year) and the absence of clearly malignant ccRCC lesions. To attempt to accelerate the formation of precursor lesions and potentially generate a mouse model that progresses to ccRCC we combined these three genotypes to reproduce the mutational and cellular changes that are found in some cases of human ccRCC. We found that the triple loss of *Vhl*, *Kif3a* and *Trp53* in mouse renal epithelia results in a variety of simple and atypical cystic lesions and neoplasms but is also insufficient to cause ccRCC. In the cyst-dependent pathway of ccRCC progression simple cysts are believed to become atypical cysts that first develop micro-foci that resemble ccRCC and these then progress to form malignant ccRCC tumours. The increased rate of cyst formation, the increased proportion of cysts with proliferating cells, the higher frequency of atypical cysts as well as the development of neoplasms in $Kif3a^{\Delta/\Delta};Vhl^{\Delta/\Delta};Trp53^{\Delta/\Delta}$ compared to $Kif3a^{\Delta/\Delta};Trp53^{\Delta/\Delta}$ mice indicates that primary cilium loss in addition to *Vhl* and *Trp53* loss promotes the transition towards malignancy.

Notably, kidneys of $Kif3a^{\Delta/\Delta};Vhl^{\Delta/\Delta};Trp53^{\Delta/\Delta}$ mice 10 months after gene deletion not only displayed cystic lesions but also displayed many histologically normal tubules in which some renal epithelial cells exhibited nuclear accumulation of HIF-1α, indicative of gene deletion in

these cells during the period of tamoxifen feeding. Thus, the combination of triple loss of *Vhl*, *Kif3a* and *Trp53* does not automatically cause cyst formation even after a long time period. This could be explained by the slow cell-turnover of the kidney tissue [26] and by findings showing that cyst formation following loss of the primary cilium requires cellular turnover [23, 27].

Our data demonstrate that loss of the primary cilium is not a strong driver of oncogenic transformation, even in a genetic background that is prone to form renal tumours. By inference, we argue that loss of the primary cilium acts as an important driver of the initiation of proliferation of *VHL* mutant cells to form precursor lesions in human kidneys, providing an expanded pool of proliferating cells that can subsequently accumulate mutations that cooperate with *VHL* mutation to fully transform renal epithelial cells and drive the formation of ccRCC. In this context, recent large-scale sequencing studies have identified frequent mutations in several tumour suppressor genes located on human chromosome 3p such as *PBRM1*, *SETD2* and *BAP1* [2, 15]. Interestingly, deletion of *Vhl* combined with heterozygous loss of *Bap1* has been shown to produce not only cystic lesions but also small renal tumours that reproduce some, but not all, of the histological and molecular features of human ccRCC [28]. After several decades of trying, ccRCC remains one of the few human tumours for which there is still no adequate autochthonous mouse model that fully reproduces the histological and clinical features of the disease, demonstrating that the molecular causes of the formation of this tumour type have not yet been fully elucidated.

In summary, we have developed a mouse model that recapitulates a variety of pre-malignant lesions that occur in the formation of ccRCC tumours in humans as well as further validated the use of contrast-assisted μCT imaging for the longitudinal monitoring of renal cystic

phenotypes. This mouse model will be useful for testing therapeutic strategies that could be employed to prevent the emergence of precursor lesions and ccRCC tumours in VHL patients.

Acknowledgements

This work was supported by grants to I.J. Frew from SNF Förderungsprofessur (PP00P3_128257) and ERC Starting Grant (260316).

Author contribution statement

AG performed data collection, data analysis and manuscript preparation. HL performed study design and mice crossings. PJW performed data collection. IJF performed study design, data collection, data analysis and manuscript preparation.

Supporting Information

The following supporting information may be found in the online version of this article.

Figure S1 PBRM1 expression and a functional readout of SETD2 activity are not altered in the renal lesions.

Supplementary Information. Primer sequences and legend for Figure S1.

References

1. Eble JN, Sauter G, Epstein JI, *et al.* Tumours of the Kidney, World Health Organization Classification of Tumours. Pathology and Genetics of Tumours of the urinary System and Male Genital Organs. *IARC Press* 2004.
2. Sato Y, Yoshizato T, Shiraishi Y, *et al.* Integrated molecular analysis of clear-cell renal cell carcinoma. *Nat Genet* 2013; **45**: 860-867.
3. Frew IJ, Moch H. A clearer view of the molecular complexity of clear cell renal cell carcinoma. *Annu Rev Pathol* 2015; **10**: 263-289.
4. Kaelin WG, Jr. Molecular basis of the VHL hereditary cancer syndrome. *Nat Rev Cancer* 2002; **2**: 673-682.
5. Maher ER, Kaelin WG, Jr. von Hippel-Lindau disease. *Medicine (Baltimore)* 1997; **76**: 381-391.
6. Choyke PL, Glenn GM, Walther MM, *et al.* The natural history of renal lesions in von Hippel-Lindau disease: a serial CT study in 28 patients. *AJR Am J Roentgenol* 1992; **159**: 1229-1234.
7. Montani M, Heinimann K, von Teichman A, *et al.* VHL-gene deletion in single renal tubular epithelial cells and renal tubular cysts: further evidence for a cyst-dependent progression pathway of clear cell renal carcinoma in von Hippel-Lindau disease. *Am J Surg Pathol* 2010; **34**: 806-815.
8. Thoma CR, Frew IJ, Krek W. The VHL tumor suppressor: riding tandem with GSK3beta in primary cilium maintenance. *Cell Cycle* 2007; **6**: 1809-1813.
9. Iliopoulos O, Kibel A, Gray S, *et al.* Tumour suppression by the human von Hippel-Lindau gene product. *Nat Med* 1995; **1**: 822-826.
10. Mandriota SJ, Turner KJ, Davies DR, *et al.* HIF activation identifies early lesions in VHL kidneys: evidence for site-specific tumor suppressor function in the nephron. *Cancer Cell* 2002; **1**: 459-468.

11. Berbari NF, O'Connor AK, Haycraft CJ*, et al.* The primary cilium as a complex signaling center. *Curr Biol* 2009; **19**: R526-535.

12. Davenport JR, Yoder BK. An incredible decade for the primary cilium: a look at a once-forgotten organelle. *Am J Physiol Renal Physiol* 2005; **289**: F1159-1169.

13. Thoma CR, Frew IJ, Hoerner CR*, et al.* pVHL and GSK3beta are components of a primary cilium-maintenance signalling network. *Nat Cell Biol* 2007; **9**: 588-595.

14. Schraml P, Frew IJ, Thoma CR*, et al.* Sporadic clear cell renal cell carcinoma but not the papillary type is characterized by severely reduced frequency of primary cilia. *Mod Pathol* 2009; **22**: 31-36.

15. Comprehensive molecular characterization of clear cell renal cell carcinoma. *Nature* 2013; **499**: 43-49.

16. Frew IJ, Thoma CR, Georgiev S*, et al.* pVHL and PTEN tumour suppressor proteins cooperatively suppress kidney cyst formation. *EMBO J* 2008; **27**: 1747-1757.

17. Lin F, Hiesberger T, Cordes K*, et al.* Kidney-specific inactivation of the KIF3A subunit of kinesin-II inhibits renal ciliogenesis and produces polycystic kidney disease. *Proc Natl Acad Sci U S A* 2003; **100**: 5286-5291.

18. Lehmann H, Vicari D, Wild PJ*, et al.* Combined Deletion of Vhl and Kif3a Accelerates Renal Cyst Formation. *J Am Soc Nephrol* 2015; **26**: 2778-2788.

19. Albers J, Rajski M, Schonenberger D*, et al.* Combined mutation of Vhl and Trp53 causes renal cysts and tumours in mice. *EMBO Mol Med* 2013; **5**: 949-964.

20. Gerlinger M, Horswell S, Larkin J*, et al.* Genomic architecture and evolution of clear cell renal cell carcinomas defined by multiregion sequencing. *Nat Genet* 2014; **46**: 225-233.

21. Shao X, Somlo S, Igarashi P. Epithelial-specific Cre/lox recombination in the developing kidney and genitourinary tract. *J Am Soc Nephrol* 2002; **13**: 1837-1846.

22. Almajdub M, Magnier L, Juillard L*, et al.* Kidney volume quantification using contrast-enhanced in vivo X-ray micro-CT in mice. *Contrast Media Mol Imaging* 2008; **3**: 120-126.

23. Patel V, Li L, Cobo-Stark P*, et al.* Acute kidney injury and aberrant planar cell polarity induce cyst formation in mice lacking renal cilia. *Hum Mol Genet* 2008; **17**: 1578-1590.

24. Bell PD, Fitzgibbon W, Sas K*, et al.* Loss of primary cilia upregulates renal hypertrophic signaling and promotes cystogenesis. *J Am Soc Nephrol* 2011; **22**: 839-848.

25. Boehlke C, Kotsis F, Patel V*, et al.* Primary cilia regulate mTORC1 activity and cell size through Lkb1. *Nat Cell Biol* 2010; **12**: 1115-1122.

26. Rinkevich Y, Montoro DT, Contreras-Trujillo H*, et al.* In vivo clonal analysis reveals lineage-restricted progenitor characteristics in mammalian kidney development, maintenance, and regeneration. *Cell Rep* 2014; **7**: 1270-1283.

27. Piontek K, Menezes LF, Garcia-Gonzalez MA*, et al.* A critical developmental switch defines the kinetics of kidney cyst formation after loss of Pkd1. *Nat Med* 2007; **13**: 1490-1495.

28. Wang SS, Gu YF, Wolff N*, et al.* Bap1 is essential for kidney function and cooperates with Vhl in renal tumorigenesis. *Proc Natl Acad Sci U S A* 2014; **111**: 16538-16543.

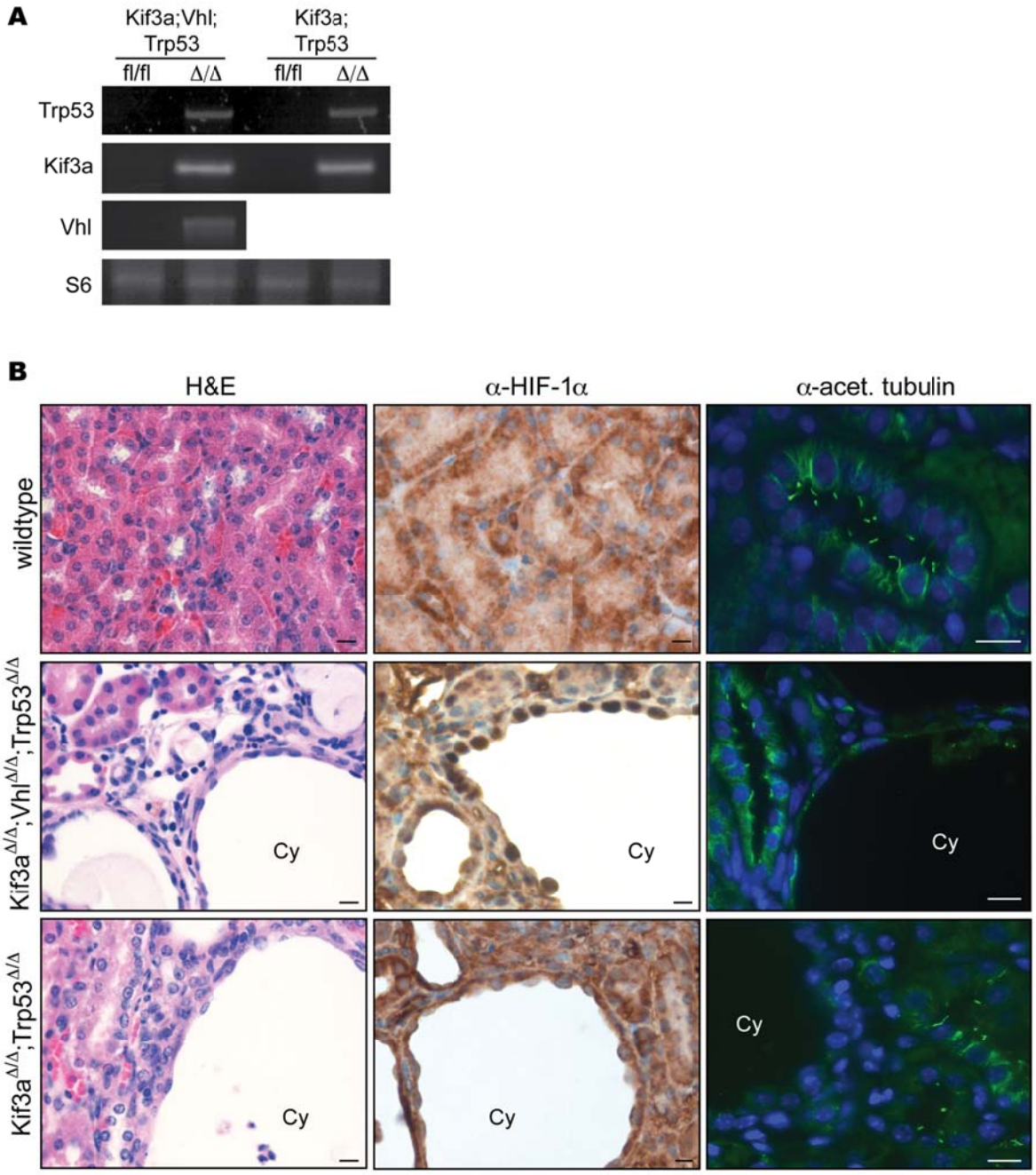

Figure 1. Generation of mice allowing inducible deletion of *Kif3a/Vhl/Trp53* or *Kif3a/Trp53*. (A) PCR from genomic DNA of kidneys from $Kif3a^{fl/fl};Vhl^{fl/fl};Trp53^{fl/fl}$, $Kif3a^{\Delta/\Delta};Vhl^{\Delta/\Delta};Trp53^{\Delta/\Delta}$, $Kif3a^{fl/fl};Trp53^{fl/fl}$ and $Kif3a^{\Delta/\Delta};Trp53^{\Delta/\Delta}$ mice. Specific primers

for the floxed (fl) and recombined (Δ) alleles were used. The promoter region of ribosomal protein S6 (S6) acted as internal DNA quality and PCR control. (B) Representative images of H&E, anti-HIF-1α and anti-acetylated tubulin immunostainings of normal and cystic (Cy) kidney regions of Kif3a$^{\Delta/\Delta}$;Vhl$^{\Delta/\Delta}$;Trp53$^{\Delta/\Delta}$ and Kif3a$^{\Delta/\Delta}$;Trp53$^{\Delta/\Delta}$ mice. H&E, haematoxylin and eosin. Scale bars, 20 μM.

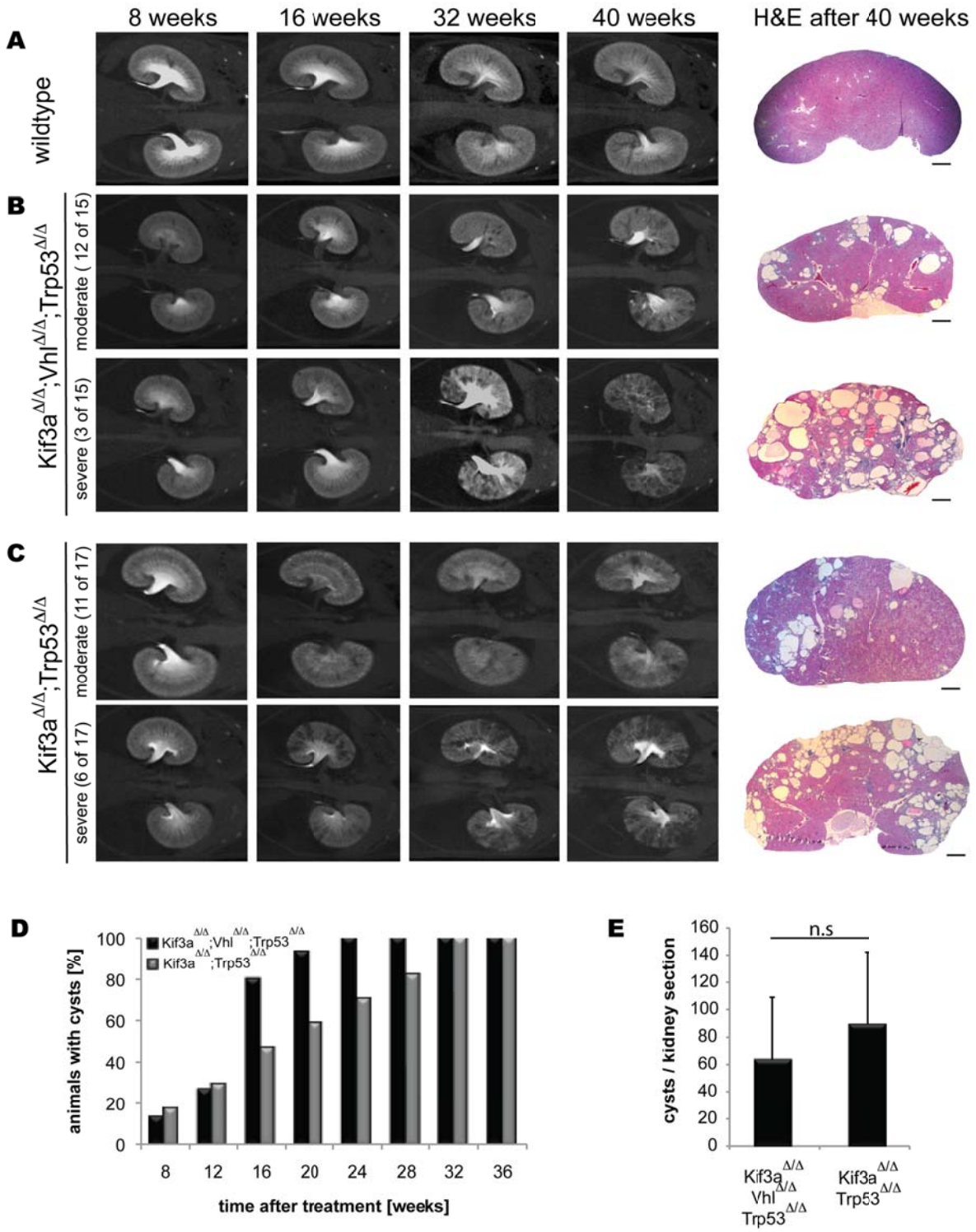

Figure 2. µCT imaging and quantitative assessment of cyst development. Representative µCT images of wildtype (A), Kif3a$^{\Delta/\Delta}$;Vhl$^{\Delta/\Delta}$;Trp53$^{\Delta/\Delta}$ (B) and Kif3a$^{\Delta/\Delta}$;Trp53$^{\Delta/\Delta}$ (C) mouse kidneys at 8, 16, 32 and 40 weeks post-tamoxifen treatment (left). Corresponding

representative histological section of each of the imaged mice at 40 weeks (right). The cystic phenotypes were visually classified as moderate or severe. H&E, haematoxylin and eosin. Scale bars, 1 mm in H&E images. (D) Percentages of animals with visually recognisable cysts in µCT images at different timepoints after tamoxifen treatment. Kif3a$^{\Delta/\Delta}$;Vhl$^{\Delta/\Delta}$;Trp53$^{\Delta/\Delta}$ (n=15) and Kif3a$^{\Delta/\Delta}$;Trp53$^{\Delta/\Delta}$ (n=17). (E) Number of cysts per kidney section established after visual analysis of histological sections. Mean ± SEM of Kif3a$^{\Delta/\Delta}$;Vhl$^{\Delta/\Delta}$;Trp53$^{\Delta/\Delta}$ (n=15) and Kif3a$^{\Delta/\Delta}$;Trp53$^{\Delta/\Delta}$ (n=23). n.s, not significant (P>0.05, Student's unpaired t test).

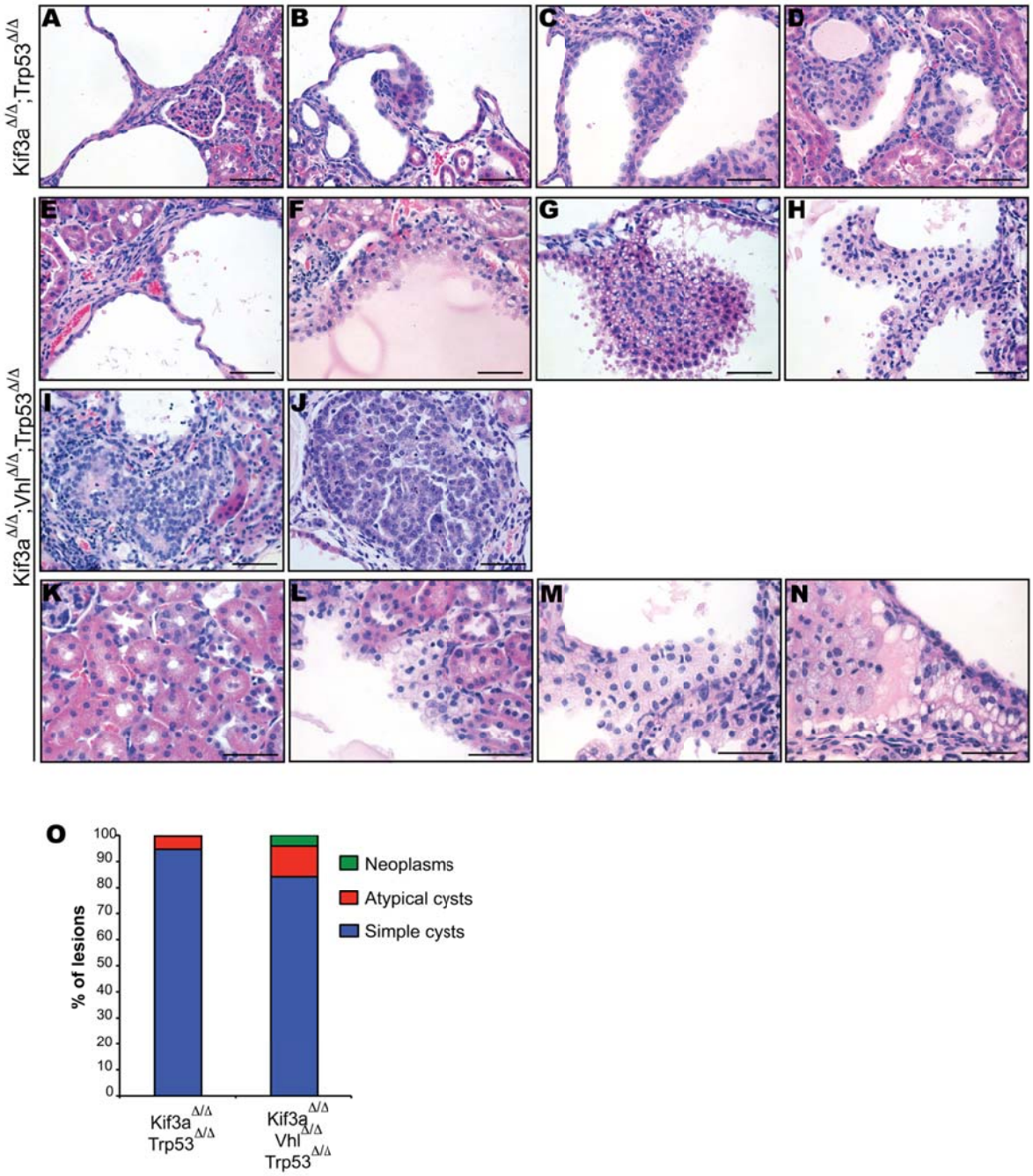

Figure 3. Kif3a$^{\Delta/\Delta}$;Vhl$^{\Delta/\Delta}$;Trp53$^{\Delta/\Delta}$ mice develop neoplasms and more atypical cysts than Kif3a$^{\Delta/\Delta}$;Trp53$^{\Delta/\Delta}$ animals. (A-D) Representative H&E stainings of a simple cyst (A), atypical cysts (B, C) and a very small neoplasm (D) from Kif3a$^{\Delta/\Delta}$;Trp53$^{\Delta/\Delta}$ mice. (E-J) Representative H&E stainings of a simple cyst (E), atypical cyst (F), neoplastic cysts (G and H)

and solid neoplasms (I and J) from Kif3a$^{\Delta/\Delta}$;Vhl$^{\Delta/\Delta}$;Trp53$^{\Delta/\Delta}$ mice. (K-N) Representative H&E stainings of normal renal tubules (K) and clear cells in an atypical cyst (L), neoplastic cyst (M) and solid neoplasm (N). (O) Proportions of the different types of lesions scored by analysis of histological sections. Kif3a$^{\Delta/\Delta}$;Vhl$^{\Delta/\Delta}$;Trp53$^{\Delta/\Delta}$ (n=15 mice) and Kif3a$^{\Delta/\Delta}$;Trp53$^{\Delta/\Delta}$ (n=23 mice). Scale bars, 50 μM.

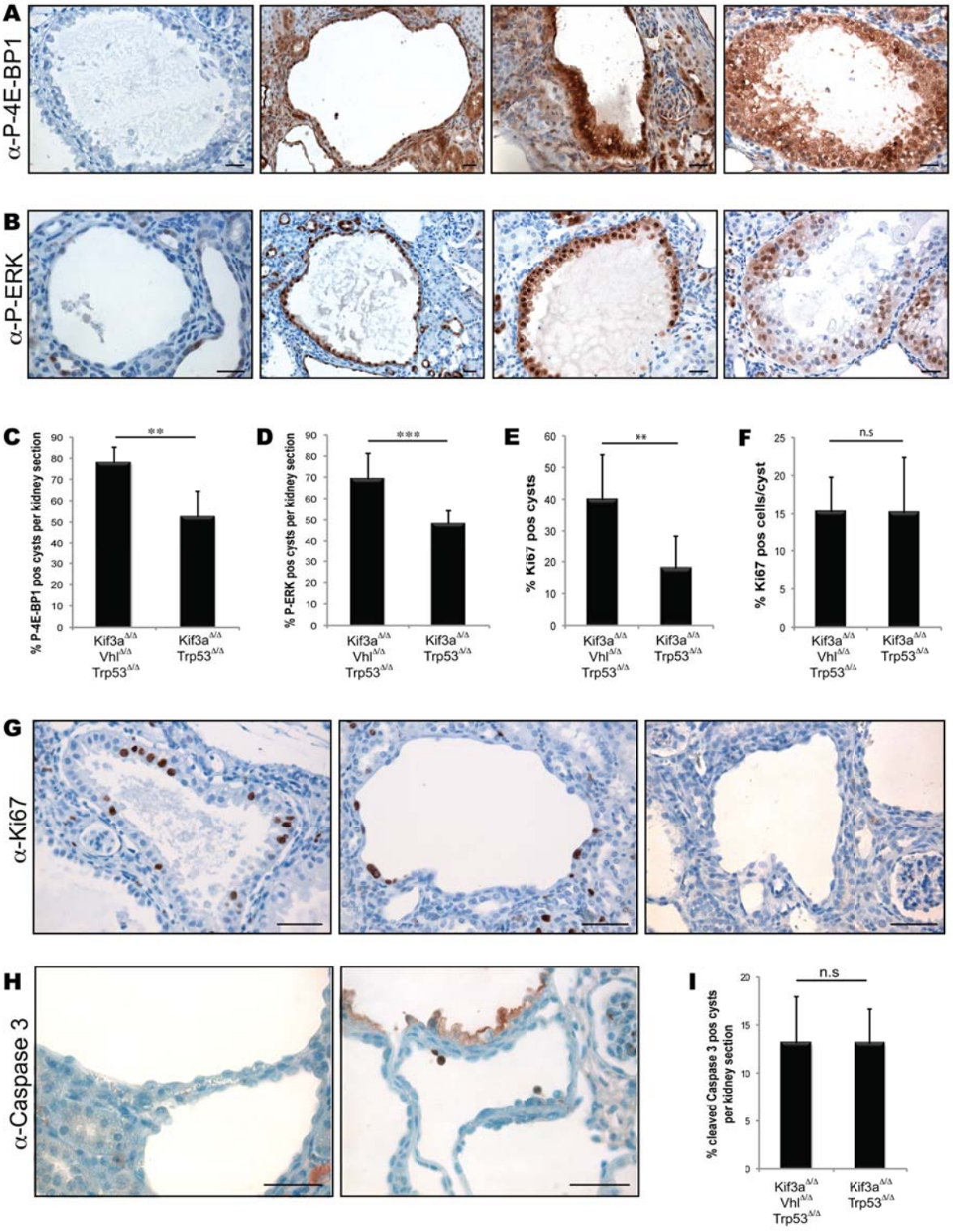

Figure 4. Kif3a$^{\Delta/\Delta}$;Vhl$^{\Delta/\Delta}$;Trp53$^{\Delta/\Delta}$ mice have more proliferating cysts than Kif3a$^{\Delta/\Delta}$;Trp53$^{\Delta/\Delta}$ animals. (A) Representative negative and positive staining of P-4E-BP1 (Thr37/46) in a simple cyst, and positive staining in an atypical cyst and neoplasm (left to

right) from Kif3a$^{\Delta/\Delta}$;Vhl$^{\Delta/\Delta}$;Trp53$^{\Delta/\Delta}$ mice. (B) Representative negative and positive staining of P-ERK1/2 (Thr202/Tyr204) in a simple cyst and positive staining in an atypical cyst and neoplasm (left to right) from Kif3a$^{\Delta/\Delta}$;Vhl$^{\Delta/\Delta}$;Trp53$^{\Delta/\Delta}$ mice. (C-E) Frequency of P-4E-BP1 positive cysts (C), P-ERK1/2 positive cysts (D) and cysts containing Ki67+ cells (E) per kidney section. Mean ± SEM of Kif3a$^{\Delta/\Delta}$;Vhl$^{\Delta/\Delta}$;Trp53$^{\Delta/\Delta}$ (n=10 mice) and Kif3a$^{\Delta/\Delta}$;Trp53$^{\Delta/\Delta}$ (n=10 mice). ** P<0.01; *** P<0.001 (Student's unpaired t test). (F) Percentage of Ki67+ cells per Ki67+ cyst. Mean ± SEM of Kif3a$^{\Delta/\Delta}$;Vhl$^{\Delta/\Delta}$;Trp53$^{\Delta/\Delta}$ (n=25 cysts) and Kif3a$^{\Delta/\Delta}$;Trp53$^{\Delta/\Delta}$ (n=26 cysts). n.s, not significant (P>0.05, Student's unpaired t test). (G) Representative positive (left and middle) and negative (right) Ki67 immunostainings of kidney cysts. (H) Representative negative (left) and positive (right) cleaved Caspase 3 immunostainings of kidney cysts. Scale bars, 50 µM. (I) Percentages of cysts containing cleaved Caspase 3 positive cells. Mean ± SEM of Kif3a$^{\Delta/\Delta}$;Vhl$^{\Delta/\Delta}$;Trp53$^{\Delta/\Delta}$ (n=10) and Kif3a$^{\Delta/\Delta}$;Trp53$^{\Delta/\Delta}$ (n=10). n.s, not significant (P>0.05, Student's unpaired t test). Scale bars, 50 µM.